

A COMPARATIVE STUDY OF MoS₂ NANOSTRUCTURES GROWN ON GLASS AND ALUMINA SUBSTRATES BY METAL-ORGANIC CHEMICAL VAPOR DEPOSITION (MOCVD) METHOD

Manh Hung Nguyen^{1,*}, Van Hoang Nguyen¹, Tien Hiep Nguyen¹,
Xuan Hung Dinh², Dinh Phong Phung³, Tien Hung Pham⁴

¹Department of Materials Science and Engineering, Le Quy Don Technical University, Hanoi, Vietnam

²Chien Thang One Member Limited Liability Company, Hanoi, Vietnam

³Office of Academic Affairs (OAA), Le Quy Don Technical University, Hanoi, Vietnam

⁴Department of Physics, Le Quy Don Technical University, Hanoi, Vietnam

Abstract

MoS₂ is one of the most attractive transition metal dichalcogenide (TMD) materials for electronic applications due to its unique properties. In this study, MoS₂ nanoflakes were synthesized by the metal-organic chemical vapor deposition (MOCVD) method on various substrates including glass and alumina. The substrate effects on the morphology and structural properties of MoS₂ nanostructures were evaluated by different techniques including field-emitting scanning electron microscope (FE-SEM), energy dispersive spectrum (EDS), X-ray diffraction (XRD), photoluminescence and Raman spectra. The results indicate that MoS₂ nanoflakes could be synthesized effectively on both glass (MoS₂/glass) and alumina (MoS₂/Al₂O₃) substrates. However, the morphology and many structural properties of MoS₂ nanoflakes are modified significantly when changing the substrates. The Mo/S atomic ratio changes from 0.62 to 0.45 for MoS₂/Al₂O₃ and MoS₂/glass, respectively. In addition, MoS₂/Al₂O₃ reveals a less uniform structure along with thicker edges of MoS₂ nanoflakes in comparison to that of MoS₂/glass. For application, as-synthesized MoS₂ nanoflakes could be considered as a potential candidate for selective H₂S detection owing to the presence of dangling bonds in MoS₂ nanoflakes as well as the differences in the adsorption ability and charge transfer between target gases and MoS₂.

Keywords: MoS₂ nanoflake; chemical vapor deposition; dangling bond.

1. Introduction

Transition metal dichalcogenide materials (general formula MX₂, where M is a transition metal (Mo, W, Sn, etc.) and X is a chalcogen element (S, Se, etc.)) have attracted much attention owing to their unique properties. Among them, MoS₂ has been proven to be a potential candidate for various applications, including gas sensors [1], photoelectrochemical (PEC) water splitting [2], and solar cells [3]. Recent studies have

* Email: hungnm@lqdtu.edu.vn

indicated that the properties of MoS₂ strongly depend on its morphological and structural characteristics, such as the thickness of MoS₂, the morphology (single layer, multilayer, nano-flake, nanowire...), the defect level of MoS₂, etc. Dong-Bum Seo et al. have found out the deposition of MoS₂ thin film on TiO₂ nanorods can promote photo-generated electron-hole separation owing to the formation of a p-MoS₂/n-TiO₂ heterojunction. The authors have also indicated that the photo-current is significantly reduced when MoS₂ thickness is large enough. The decrease of photo-current is originated from a strong electron-hole recombination in thick MoS₂ layer [2]. In addition, for gas-sensing applications, theoretical and experimental studies suggest that intrinsic point defect (vacancy) is an important factor that controls the sensing behavior of MoS₂. Sulfur-vacancy-enriched MoS₂ nanosheets displayed a better NO₂-sensing performance compared to pure MoS₂ nanosheets [4]. Similarly, doping is also an effective way to improve the sensing properties of MoS₂ by altering the binding configurations with the presence of substitution/interstitial atoms [5]. Along with structural defects, the morphological effect of MoS₂ was reported by Kun Hong Hu and his colleagues. The authors have recognized the large differences in catalytic properties and lubrication ability between MoS₂ nano-slices and MoS₂ nano-balls [6]. From these studies, it is recognized that the synthesis procedure of MoS₂ strongly affects its morphological and intrinsic properties, thereby affecting the applications that MoS₂ is used. Therefore, scientists have proposed various methods for the synthesis of different MoS₂ nanostructures with desired properties, such as hydrothermal [7], chemical vapor deposition [8], Au-assisted exfoliation [9], atomic layer deposition (ALD) [10], and metal-organic chemical vapor deposition (MOCVD) [11, 12]. Along with synthesis methods, the substrate was also identified to be an important factor that significantly affects the performance of MoS₂. Changing substrate results in the significant changes in the properties of MoS₂, including charge carrier mobility [13], uniform [14], morphology [15], crystalline quality, built-in strain and charge doping [16]. Woo Hyun Chae et al. have investigated the MoS₂ growth on four substrates: boron nitride, SiO₂/Si, sapphire, and muscovite mica. They have suggested that the built-in strain and charge doping increase when the substrates become more rough [16]. Clearly, the substrate effect should be considered carefully for growth of MoS₂. However, while many researches on the substrate effect on MoS₂ monolayer have been reported, there are few such reports toward multi-layer MoS₂. Based on such considerations, we have investigated the substrate effect on the morphology and properties of MoS₂ nanoflakes synthesized by MOCVD method. This study aims to evaluate and compare the growth

ability of MoS₂ nanoflakes on various substrates including glass and alumina. In addition, we have also examined the gas-sensing performance of prepared MoS₂ nanoflakes as an illustration for one of potential applications of MoS₂ nanoflakes.

2. Experiment

The reagents Mo(CO)₆ (6N purity level) and H₂S gas (5 vol% in balance N₂) were purchased from Sigma-Aldrich Co., Ltd. (USA) and NK Co., Ltd. (Korea), respectively. For the synthesis of MoS₂ nanoflakes, ordinary glass (glass) and alumina substrates (2.5 cm x 2.5 cm) were cleaned many times by acetone, ethanol, and DI water in an ultrasonicator and dried by N₂ gas. In this study, the roughness of the alumina substrate is much larger than that of the glass substrate as shown in Fig. 3. Then these substrates were placed into a quartz tube of a MOCVD system. Mo(CO)₆ and H₂S gas were used as precursors for the formation of Mo and S atoms during the growth process. Mo(CO)₆ bottle was remained at 20°C to ensure Mo(CO)₆ was vaporized stably. Mo(CO)₆ vapor was mixed with H₂S with a ratio of 1:3, while the total flow was maintained at 100 standard cubic centimeters per minute (sccm). In this study, MoS₂ nanoflakes were grown at a temperature of 250°C, which was optimized to obtain the best uniform of MoS₂. For comparison, the deposition time was controlled similarly for the growth processes on both alumina and glass substrates (Fig. 1). The alumina and glass substrates deposited MoS₂ nanoflakes are denoted as MoS₂/Al₂O₃ and MoS₂/glass, respectively.

Morphologies of MoS₂ flakes were observed by scanning electron microscopy (SEM, Hitachi S4800, Japan), while the composition was analyzed by energy-dispersive spectrum (EDS) integrated with SEM equipment. Raman and photoluminescence (PL) spectra were conducted at room temperature using an excitation wavelength of 532 nm. The crystalline structures of MoS₂ samples were examined by X-ray diffraction with Cu-K α radiation (0.1540598 μ m) using Bragg-Brentano geometry.

The sensors were fabricated by depositing Pt comb electrodes on the surfaces of the corresponding substrates using a direct current (DC) sputtering technique and a shadow mask (Fig. 1). The sensing properties of MoS₂/Al₂O₃- and MoS₂/glass-based sensors were examined by a homemade gas-sensing measurement system. The target gases (CO, H₂, NH₃, CH₄, H₂S, NO₂) and dry air (approximately 21% O₂ and 79% N₂) were mixed to create different concentrations of the target gases using mass flow controllers (MFCs). The response (S) of the sensor was calculated by $S = R_g/R_a$ or $S = R_a/R_g$ for reducing and oxidizing gases, respectively. Herein, R_g is ascribed to the resistance of the sensor in the mixture of dry air and target gas, while R_a is the resistance of the sensor in dry air.

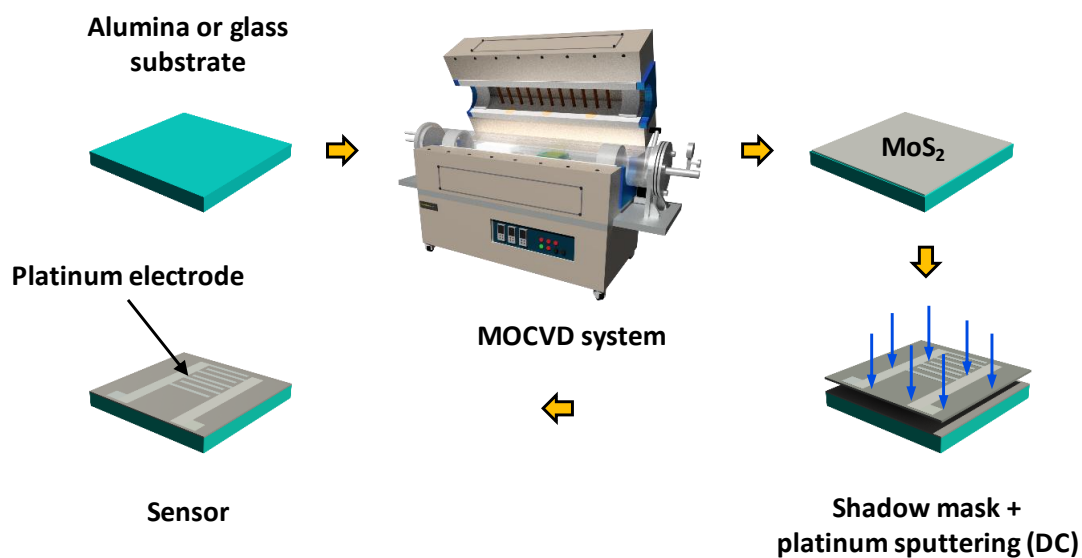


Fig. 1. A schematic illustration of MoS₂ deposition process and fabrication of MoS₂ sensor.

3. Results and discussions

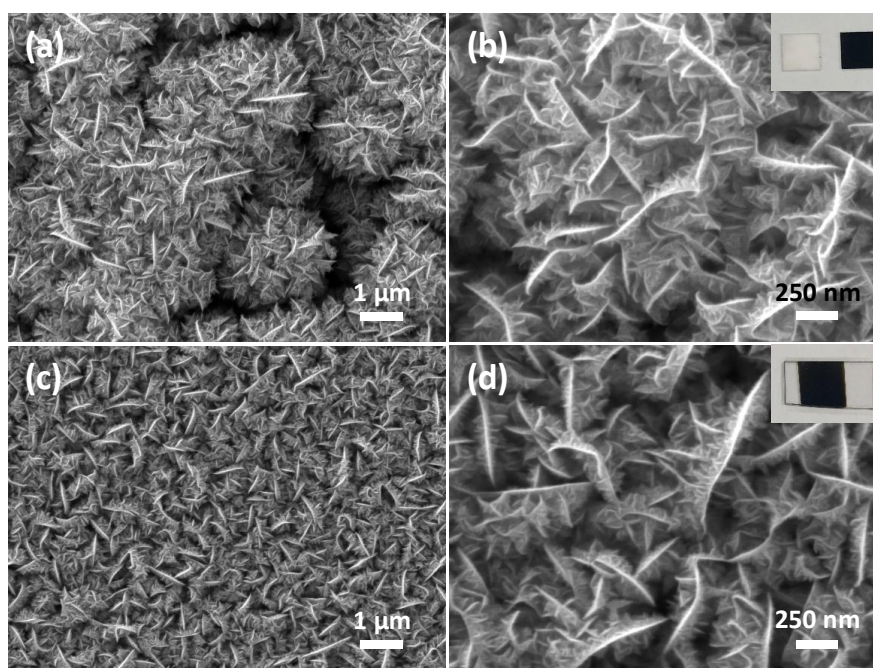


Fig. 2. SEM images with different magnifications of MoS₂ grown on (a, b) alumina and (c, d) glass substrates. The inset in figure (b) shows alumina substrate before (white) and after (black) deposition of MoS₂. The inset in figure (d) is a photograph of the glass substrate with the MoS₂ part grown in the middle (black part).

The insets in Fig. 2 (b, d) show that MoS₂ can be easily grown on both alumina and glass substrates. The color of the alumina substrate is changed from white to black after the deposition of MoS₂. A similar result is also observed on the glass substrate (the inset in Fig. 2(d)). The middle part of the glass substrate is black owing to the formation of the MoS₂ layer, while the white part is the pristine glass substrate. SEM images of MoS₂/Al₂O₃ and MoS₂/glass display nanoflake morphology of deposited MoS₂ on both substrates. However, MoS₂ nanoflakes grown on alumina substrate are accumulated into MoS₂ clusters, while those grown on glass exhibit a better uniformity (Fig. 2(a, c)). The high roughness of the alumina substrate is responsible for the low uniformity of the MoS₂ layer as well as the formation of the MoS₂ clusters. At a higher magnification, it is found out that the dimensions of flakes on alumina and glass are similar. For gas-sensing applications, it is worth noting that the presence of many large gaps between clusters is a favorable factor for the diffusion of target gas molecules to the MoS₂ layers underneath the surface, thereby increasing the interaction between the sensing material and the target gas molecules. As a result, a higher response is expected for MoS₂/Al₂O₃ compared to MoS₂/glass.

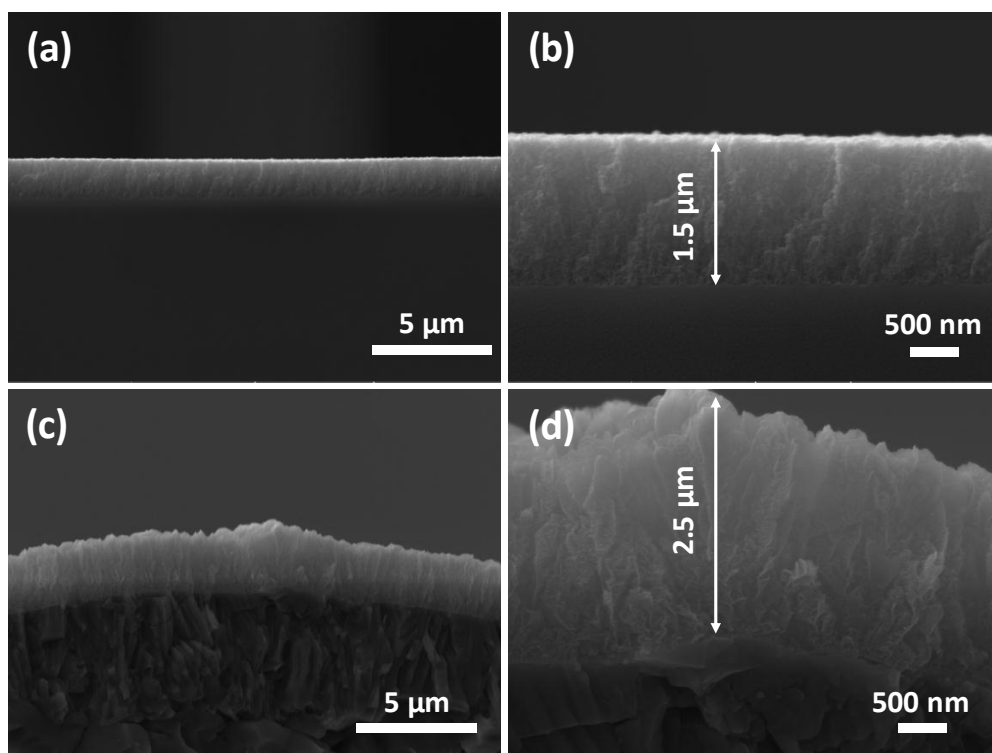


Fig. 3. Cross-sectional SEM images with different magnifications of MoS₂ grown on (a, b) glass and (c, d) alumina substrates.

The cross-sectional image in Fig. 3(a) indicates the excellent uniformity of the MoS₂ layer grown on the glass substrate. The thickness of the MoS₂ layer is almost unchanged throughout the observed length in Fig. 3(a). On the contrary, the MoS₂/Al₂O₃ reveals a poor uniformity (Fig. 3(c)). These observations can be explained by the large difference in the roughness between glass and alumina substrates. It also should be noted that glass substrate possesses an amorphous lattice structure, while alumina substrate is polycrystalline (as shown in XRD results in Fig. 5(a)). These results exhibit that MoS₂ nanoflakes could be grown easily on both amorphous and crystalline substrates. However, the nature of substrates strongly affects the growth rate of MoS₂, thereby the thickness of the obtained MoS₂ nanoflakes layer. The thickness of the MoS₂ nanoflakes layer grown on Al₂O₃ substrate is approximately 1.5 times greater than that of MoS₂/glass while depositing conditions are similar. In addition, the lower uniformity of MoS₂/Al₂O₃ along the thickness in comparison to MoS₂/glass is further confirmed in Fig. 3. The below part of the MoS₂/Al₂O₃ layer reveals small flakes along with a low porosity. In contrast, the upper part shows large MoS₂ nanoflakes with a high porosity (Fig. 3(d)). In the meantime, the uniform morphology and porosity of MoS₂/glass nanoflakes could be observed in cross-sectional SEM images in Figures 3(a, b). Generally, the substrate effect on the thickness and morphology of MoS₂ is significant, therefore the substrate needs to be chosen carefully for the various applications of MoS₂.

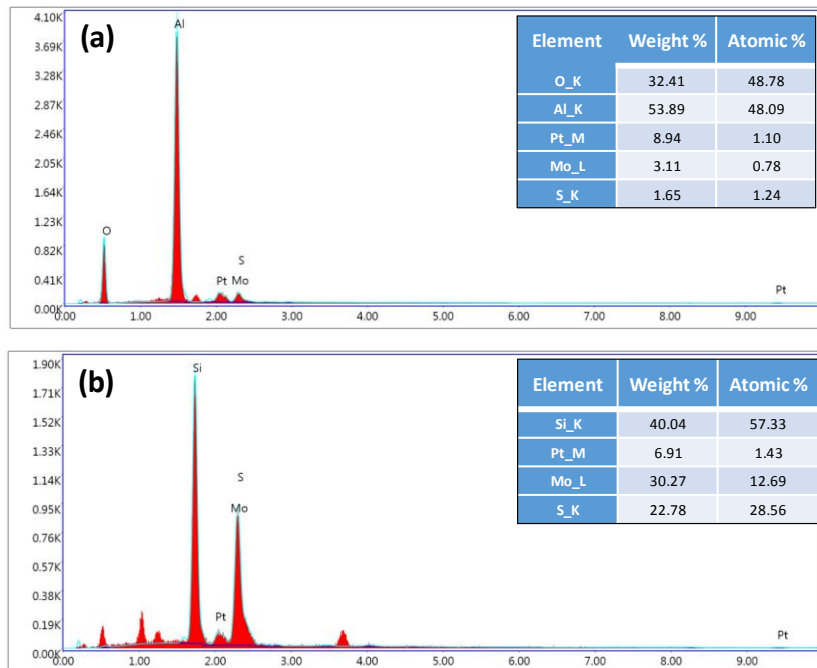


Fig. 4. EDS spectra of (a) MoS₂/Al₂O₃ and (b) MoS₂/glass.

In order to consider the substrate effect on the chemical composition of deposited MoS₂ samples, energy-dispersive spectra (EDS) were recorded. Fig. 4 shows the EDS of MoS₂/Al₂O₃ and MoS₂/glass. The atomic Mo/S ratio of MoS₂/Al₂O₃ is approximately 0.62, while that of MoS₂/glass is 0.45. These results suggest that MoS₂/Al₂O₃ is S deficiency, while MoS₂/glass is Mo deficiency. Clearly, the role of the substrate is very important when MoS₂ is grown by the MOCVD method. The substrate not only affects the morphology of MoS₂ as discussed above but also changes the chemical composition of MoS₂. The Mo or S deficiencies lead to significant changes in the various properties of MoS₂, such as charge density [17], electronic structure [18], gas adsorption ability owing to the formation of dangling bonds [19]. Therefore, this observation also paves a simple way to synthesize MoS₂ with desired composition, morphology, and properties for different applications. Fig. 5(a) shows X-ray diffraction spectra of MoS₂/Al₂O₃ and MoS₂/glass. Diffraction peaks at 13.87, 32.96, 38.75, and 59.08 are ascribed to lattice planes (002), (100), (103), and (110) of MoS₂/glass [20]. In the meantime, only one peak (002) of MoS₂ is observed on the alumina substrate. It is worth mention that alumina substrate is comprised of lattice phases while glass is amorphous. This thing results in only one peak observed in the XRD spectrum of MoS₂/Al₂O₃ due to the large differences in the diffraction intensity between diffraction peaks of Al₂O₃ substrate and MoS₂. In the XRD spectrum of MoS₂/glass, the presence of diffraction peak of glass substrate indicates that MoS₂/glass possesses a low crystallinity. In other words, MoS₂/Al₂O₃ nanoflakes gain a higher crystallinity than that of MoS₂/glass. But generally speaking, the crystallinities of as-synthesized MoS₂ nanoflakes on both kinds of substrate in this study are relatively low. In order to further understand the effect of the substrate on the structural properties of MoS₂, Raman spectra of MoS₂ were measured at 25°C using an excitation source of 532 nm. Characteristic Raman peaks (E_{1g} and A_{1g}) are observed in both samples (MoS₂/Al₂O₃ and MoS₂/glass). These two peaks are strongly affected by the edge thicknesses of the MoS₂ nanoflakes. The studies indicated that E_{2g} reveals a redshift when the number of the MoS₂ layer increases. In contrast, A_{1g} shows a blue shift along with the increase of MoS₂ thickness [21, 22]. In this study, such shifts were observed when the glass substrate was replaced by the alumina substrate for the MoS₂ synthesis process (Fig. 5(b)). However, it should be noted that such shifts only take place when MoS₂ thickness is about a few layers. Therefore, we believe that the observed shifts are related to the edges of MoS₂ flakes than their bulk part. In other words, the edges of MoS₂/Al₂O₃ flakes are thicker than those of MoS₂/glass.

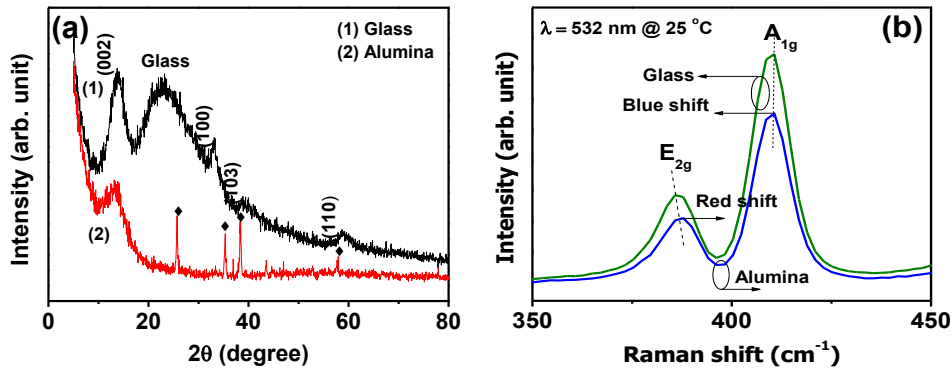


Fig. 5. (a) X-ray diffraction and (b) Raman spectra of $\text{MoS}_2/\text{Al}_2\text{O}_3$ and $\text{MoS}_2/\text{glass}$.

To further confirm the results obtained from the Raman spectrum, the photoluminescence spectrum was also measured (Fig. 6). The PL peak of $\text{MoS}_2/\text{glass}$ is observed at ~ 687 nm, while that of $\text{MoS}_2/\text{Al}_2\text{O}_3$ is at 666 nm. An approximately 20 nm shift of PL peak can be attributed to the changes in the composition of synthesized MoS_2 nanoflakes which create Mo or S vacancies. The presence of these vacancies results in changes in the electronic structure of MoS_2 , thereby changing its optical properties. F. Fabbri et al. have recognized that an excess of sulfur vacancy in MoS_2 is the root of a redshift in the PL spectrum [23]. In this study, the PL peak of $\text{MoS}_2/\text{glass}$ shows a redshift compared to that of $\text{MoS}_2/\text{Al}_2\text{O}_3$. This observation is consistent with the chemical compositions obtained from EDS (Fig. 4). In conclusion, substrate change strongly affects the morphological and structural properties of MoS_2 grown by the MOCVD technique, such as composition, edge thickness of MoS_2 nanoflakes, kind of vacancy, porosity, and uniformity. Therefore, control of MoS_2 growth through choosing suitable substrates is a potential solution to obtain desired MoS_2 properties for various applications.

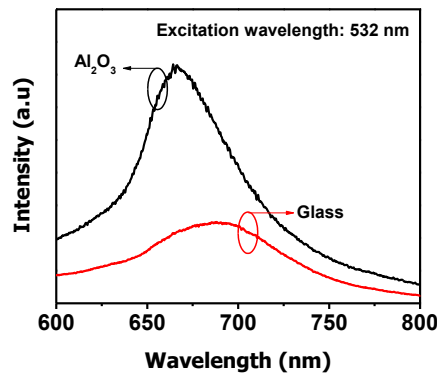


Fig. 6. Photoluminescence spectra of $\text{MoS}_2/\text{Al}_2\text{O}_3$ and $\text{MoS}_2/\text{glass}$ were measured at room temperature (25°C) using a excitation source of 532 nm.

In order to illustrate one of the various applications of MoS₂, the authors examined the sensing properties of MoS₂/Al₂O₃- and MoS₂/glass-based sensors toward various target gases, and the results are shown in Fig. 7. Both sensors show responses toward all examined target gases, including CH₄, CO, H₂, H₂S, NH₃, and NO₂. The p-type gas sensing behaviors of MoS₂ are observed in both sensors, they inferred that p-doping is predominant over n-doping in as-synthesized MoS₂ nanoflakes. P-type MoS₂ have also been reported in the literature [24, 25]. Among examined gases, the responses of the sensors toward H₂S gas are significantly faster and higher than those of other gases. This phenomenon can be attributed to the presence of Mo and S dangling bonds in defective MoS₂ nanoflakes. H₂S molecules with the presence of S atom can more favorably interact with such dangling bonds of MoS₂. In addition, this thing could also be explained by the different adsorption ability and charge transfer between target gases to defective MoS₂ nanoflakes in which H₂S possesses higher values [25]. However, similar p-type sensing behaviors of both MoS₂/Al₂O₃- and MoS₂/glass-based sensors along with different vacancies (Mo and/or S deficiency) remain a phenomenon that needs to be investigated further. The response of the MoS₂/Al₂O₃-based sensor is slightly larger in comparison to that of the MoS₂/glass-based sensor. This thing is originated from the presence of gaps between MoS₂ clusters in MoS₂/Al₂O₃, which promote the gas diffusion into the MoS₂ layers underneath the surface, thereby enhancing the gas-MoS₂ surface interaction. Generally, the gas-sensing properties indicate that MoS₂ is relatively selective for H₂S gas detection. However, the response of the MoS₂ nanoflakes-based sensor still needs to be further improved for real applications.

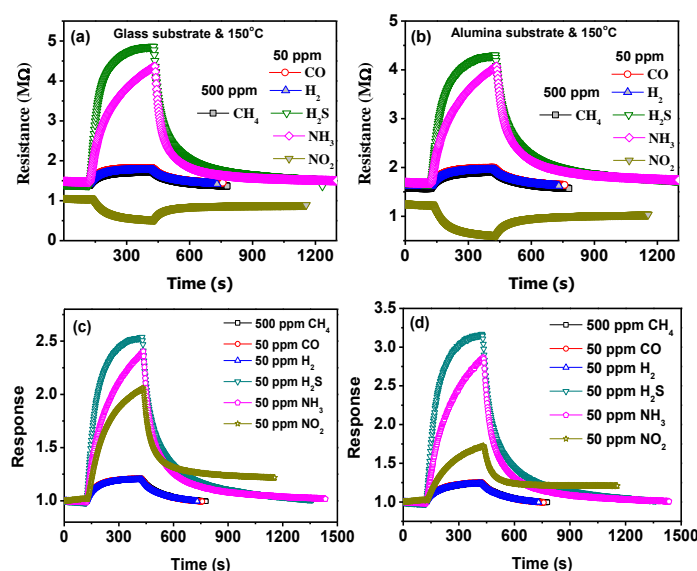


Fig. 7. Transient resistance curves of (a) MoS₂/glass- and (b) MoS₂/Al₂O₃-based sensors under the exposure of various target gases; (c) and (d) The responses of the sensors are derived from (a) and (b), respectively.

4. Conclusions

In this study, we synthesized MoS₂ nanoflakes on glass and alumina substrates and the substrate effects on morphological and structural properties were investigated. The results reveal that edge thickness, kind of vacancy, porosity, and uniformity of MoS₂ nanoflakes strongly depends on the kind of used substrate for MoS₂ growth. Gas-sensing results illustrate that MoS₂ nanoflakes can be used for selective H₂S detection due to the presence of Mo or S dangling bonds. The substrate-dependent properties of MoS₂ suggest a simple way to improve MoS₂ nanoflakes-based applications through choosing a suitable substrate for the growth of MoS₂ by MOCVD method.

Acknowledgments

The authors are thankful to Prof. Dojin Kim and Prof. Eui Tae Kim for MoS₂ synthesis and gas-sensing measurement.

References

- [1] R. Kumar, W. Zheng, X. Liu, J. Zhang, M. Kumar, "MoS₂-Based Nanomaterials for Room-Temperature Gas Sensors," *Advanced Materials Technologies*, Vol. 5, 1901062, 2020.
- [2] D.-B. Seo, S. Kim, T.N. Trung, D. Kim, E.-T. Kim, "Conformal growth of few-layer MoS₂ flakes on closely-packed TiO₂ nanowires and their enhanced photoelectrochemical reactivity," *Journal of Alloys and Compounds*, Vol. 770, 686-91, 2019.
- [3] M.-L. Tsai, S.-H. Su, J.-K. Chang, D.-S. Tsai, C.-H. Chen, C.-I. Wu, et al., "Monolayer MoS₂ Heterojunction Solar Cells," *ACS Nano*, Vol. 8, 8317-22, 2014.
- [4] Y. Xia, C. Hu, S. Guo, L. Zhang, M. Wang, J. Peng, et al., "Sulfur-Vacancy-Enriched MoS₂ Nanosheets Based Heterostructures for Near-Infrared Optoelectronic NO₂ Sensing," *ACS Applied Nano Materials*, Vol. 3, 665-73, 2020.
- [5] A. Ramanathan, "Defect Functionalization of MoS₂ nanostructures as toxic gas sensors: A review," *IOP Conference Series: Materials Science and Engineering*, IOP Publishing, 2018, p. 012001.
- [6] K.H. Hu, X.G. Hu, X.J. Sun, "Morphological effect of MoS₂ nanoparticles on catalytic oxidation and vacuum lubrication," *Applied Surface Science*, Vol. 256, 2517-23, 2010.
- [7] W.-J. Li, E.-W. Shi, J.-M. Ko, Z.-z. Chen, H. Ogino, T. Fukuda, "Hydrothermal synthesis of MoS₂ nanowires," *Journal of Crystal Growth*, Vol. 250, 418-22, 2003.
- [8] Y.-H. Lee, X.-Q. Zhang, W. Zhang, M.-T. Chang, C.-T. Lin, K.-D. Chang, et al., "Synthesis of Large-Area MoS₂ Atomic Layers with Chemical Vapor Deposition," *Advanced Materials*, Vol. 24, 2320-5, 2012.

- [9] S.E. Panasci, E. Schilirò, F. Migliore, M. Cannas, F.M. Gelardi, F. Roccaforte, et al., "Substrate impact on the thickness dependence of vibrational and optical properties of large area MoS₂ produced by gold-assisted exfoliation," *Applied Physics Letters*, Vol. 119, 093103, 2021.
- [10] J. Yang, L. Liu, "Trickle Flow Aided Atomic Layer Deposition (ALD) Strategy for Ultrathin Molybdenum Disulfide (MoS₂) Synthesis," *ACS Applied Materials & Interfaces*, Vol. 11, 36270-7, 2019.
- [11] H. Kim, D. Ovchinnikov, D. Deiana, D. Unuchek, A. Kis, "Suppressing Nucleation in Metal-Organic Chemical Vapor Deposition of MoS₂ Monolayers by Alkali Metal Halides," *Nano Letters*, Vol. 17, 5056-63, 2017.
- [12] S. Cwik, D. Mitoraj, O. Mendoza Reyes, D. Rogalla, D. Peeters, J. Kim, et al., "Direct Growth of MoS₂ and WS₂ Layers by Metal Organic Chemical Vapor Deposition," *Advanced Materials Interfaces*, Vol. 5, 1800140, 2018.
- [13] W. Bao, X. Cai, D. Kim, K. Sridhara, M.S. Fuhrer, "High mobility ambipolar MoS₂ field-effect transistors: Substrate and dielectric effects," *Applied Physics Letters*, Vol. 102, 042104, 2013.
- [14] J. Shi, X. Zhang, D. Ma, J. Zhu, Y. Zhang, Z. Guo, et al., "Substrate Facet Effect on the Growth of Monolayer MoS₂ on Au Foils," *ACS Nano*, Vol. 9, pp. 4017-4025, 2015.
- [15] H. Yin, X. Zhang, J. Lu, X. Geng, Y. Wan, M. Wu, et al., "Substrate effects on the CVD growth of MoS₂ and WS₂," *Journal of Materials Science*, Vol. 55, 990-6, 2020.
- [16] W.H. Chae, J.D. Cain, E.D. Hanson, A.A. Murthy, V.P. Dravid, "Substrate-induced strain and charge doping in CVD-grown monolayer MoS₂," *Applied Physics Letters*, Vol. 111, 143106, 2017.
- [17] Q. Zhang, X. Zhang, M. Li, J. Liu, Y. Wu, "Sulfur-deficient MoS_{2-x} promoted lithium polysulfides conversion in lithium-sulfur battery: A first-principles study," *Applied Surface Science*, Vol. 487, pp. 452-463, 2019.
- [18] S. Kc, R.C. Longo, R. Addou, R.M. Wallace, K. Cho, "Impact of intrinsic atomic defects on the electronic structure of MoS₂ monolayers," *Nanotechnology*, Vol. 25, 375703, 2014.
- [19] R.R. Kumar, M.R. Habib, A. Khan, P.-C. Chen, T. Murugesan, S. Gupta, et al., "Sulfur Monovacancies in Liquid-Exfoliated MoS₂ Nanosheets for NO₂ Gas Sensing," *ACS Applied Nano Materials*, Vol. 4, 9459-70, 2021.
- [20] X. Shan, S. Zhang, N. Zhang, Y. Chen, H. Gao, X. Zhang, "Synthesis and characterization of three-dimensional MoS₂@carbon fibers hierarchical architecture with high capacity and high mass loading for Li-ion batteries," *Journal of colloid and interface science*, Vol. 510, 327-33, 2018.
- [21] S. Golovynskyi, I. Irfan, M. Bosi, L. Seravalli, O.I. Datsenko, I. Golovynska, et al., "Exciton and trion in few-layer MoS₂: Thickness- and temperature-dependent photoluminescence," *Applied Surface Science*, Vol. 515, 146033, 2020.

- [22] S. Najmaei, Z. Liu, P.M. Ajayan, J. Lou, "Thermal effects on the characteristic Raman spectrum of molybdenum disulfide (MoS_2) of varying thicknesses," *Applied Physics Letters*, Vol. 100, 013106, 2012.
- [23] F. Fabbri, E. Rotunno, E. Cinquanta, D. Campi, E. Bonnini, D. Kaplan, et al., "Novel near-infrared emission from crystal defects in MoS_2 multilayer flakes," *Nature communications*, Vol. 7, pp. 1-7, 2016.
- [24] Y. Zhou, C. Zou, X. Lin, Y. Guo, "UV light activated NO_2 gas sensing based on Au nanoparticles decorated few-layer MoS_2 thin film at room temperature," *Applied Physics Letters*, Vol. 113, 082103, 2018.
- [25] A.V. Agrawal, R. Kumar, S. Venkatesan, A. Zakhidov, G. Yang, J. Bao, et al., "Photoactivated Mixed In-Plane and Edge-Enriched p-Type MoS_2 Flake-Based NO_2 Sensor Working at Room Temperature," *ACS Sensors*, Vol. 3, pp. 998-1004, 2018.

NGHIÊN CỨU SO SÁNH CÁC CẤU TRÚC NANO MoS_2 ĐƯỢC MỘC TRÊN CÁC ĐỀ THỦY TINH VÀ ĐỀ NHÔM ÔXIT BẰNG PHƯƠNG PHÁP LẮNG ĐỘNG PHA HƠI HÓA HỌC (MOCVD)

**Nguyễn Mạnh Hùng, Nguyễn Văn Hoàng, Nguyễn Tiến Hiệp
Đình Xuân Hùng, Phùng Đình Phong, Phạm Tiến Hưng**

Tóm tắt: MoS_2 là một trong những vật liệu dichalcogenide kim loại chuyển tiếp hấp dẫn nhất cho các ứng dụng điện tử do các tính chất đặc biệt của nó. Trong nghiên cứu này, các cụm nano MoS_2 đã được tổng hợp bằng phương pháp lắng đọng pha hơi hóa học (MOCVD) lên các loại đế khác nhau bao gồm đế nhôm ôxit và đế thủy tinh. Ảnh hưởng của đế lên hình thái và các tính chất cấu trúc của các cấu trúc nano MoS_2 đã được đánh giá bằng các kỹ thuật khác nhau bao gồm kính hiển vi điện tử phát xạ trường (FE-SEM), phổ tán sắc năng lượng (EDS), nhiễu xạ tia X, phổ huỳnh quang và phổ Raman. Các kết quả chỉ ra rằng, các MoS_2 có thể được tổng hợp hiệu quả lên cả đế thủy tinh (MoS_2 /thủy tinh) và đế nhôm ôxit (MoS_2 /nhôm ôxit). Tuy nhiên, hình thái và nhiều tính chất cấu trúc của MoS_2 bị biến đổi đáng kể khi thay đổi đế. Tỷ số nguyên tử Mo/S thay đổi tương ứng từ 0,62 tới 0,45 cho MoS_2 /thủy tinh và MoS_2 /nhôm ôxit. Thêm vào đó, MoS_2 /nhôm ôxit tiết lộ một cấu trúc đồng nhất thấp hơn cùng với các cạnh của MoS_2 dày hơn so với MoS_2 /thủy tinh. Về ứng dụng, MoS_2 đã tổng hợp có thể được xem xét như là một ứng viên tiềm năng cho phát hiện chọn lọc khí H_2S do sự hiện diện của các liên kết tự do trong MoS_2 cũng như các khác biệt trong khả năng hấp thụ và dịch chuyển điện tích giữa các khí thử và MoS_2 .

Từ khóa: Bông nano MoS_2 ; lắng đọng pha hơi hóa học; liên kết treo.

Received: 22/02/2022; Revised: 29/04/2022; Accepted for publication: 02/06/2022

